

Probing Nanoscale Dipole-Dipole Interactions by Electric Force Microscopy

T. Mélin,* H. Diesinger, D. Deresmes, and D. Stiévenard

*Institut d'Electronique de Microélectronique et de Nanotechnologie,
CNRS-UMR, 8520, Avenue Poincaré, BP 69, 59652 Villeneuve d'Ascq Cedex, France*

(Received 5 November 2003; published 20 April 2004)

We address the issue of dipole-dipole interaction measurements at the nanometer scale. Electric dipoles with tunable effective momentum in the range 10^3 – 10^4 D are generated by charge injection in single silicon nanoparticles on a conductive substrate and probed by a spectroscopic electric force microscopy analysis. Weak dipole-dipole force gradients are measured and identified from their quadratic momentum dependence. The results suggest that dipolar interactions associated with atomic-scale charge displacements or molecules can be probed by noncontact atomic force microscopy.

DOI: 10.1103/PhysRevLett.92.166101

PACS numbers: 68.37.Ps, 73.90.+f, 81.07.Bc

Dipolar interactions govern many elemental processes in the organization of matter at the nanometer scale in physics or chemistry. In molecules, dipoles of the order of a few debye originate in intramolecular charge displacements and can lead to intermolecular force fields driving the organization of molecular aggregates on flat surfaces as resolved by scanning tunneling microscopy experiments [1]. A direct control of dipolar intermolecular interactions has even been recently achieved using molecules synthesized with appropriate dipolar group locations and leading to specific self-assembling properties [2]. A dipolar behavior is also expected from semiconductor nanostructures such as CdSe nanorods, exhibiting a structural permanent dipole along their c axis with a few hundred debye moments, and enabling a collective orientation of the nanostructures in transient electric-field experiments [3]. Dipole interactions also participate in noncontact atomic force imaging mechanisms on insulator surfaces [4], and on semiconductors such as the 7×7 reconstructed (111) silicon surface, where atomic-scale charge displacements associated with surface dangling bonds induce significant image dipole moments at the tip apex [5].

All these experiments in the fields of physics and chemistry raise the question of the identification and of the measurement of dipole-dipole interactions at the nanometer scale. This issue is of fundamental interest in order to understand the reactivity or local charge transfers on surfaces and to quantify force fields between nanostructures or molecules on surfaces. We demonstrate experimentally in this Letter that dipole-dipole interactions can be identified using an atomic force microscope operated in the electric force microscopy (EFM) mode [6]. Our results suggest that electric force microscopy is very promising to measure and study the weak interactions associated with charge transfers at the nanometer scale.

To identify dipole-dipole interactions, we experimentally generate surface dipoles with tunable effective momentum in the range 10^3 – 10^4 D by charge injection in silicon nanoparticles on a conductive substrate [7,8]. The force gradients associated with the surface dipoles are

then measured by EFM measurements. From a careful analysis of EFM signals, it is shown that the dipole-dipole interactions between the surface dipoles and their cantilever tip image can be dissociated from usual dipole-charge EFM interactions [9]. The dipolar interaction is then unambiguously identified from its squared momentum dependence.

Experiments are sketched in Fig. 1. We use a silicon nanoparticle of height $h \approx 50$ nm and base radius ≈ 40 nm as charge storage node. The charge injection [8] is performed by bringing the EFM tip apex in contact with the top of a nanoparticle and biasing the tip at V_{inj} with respect to the substrate so that an amount Q of charges tunnels into the nanoparticle through its native oxide of thickness ≈ 1.5 nm [Fig. 1(a)]. The charge storage is ensured by the nanoparticle native oxide, with typical retention times of the order of 5 to 10 min [8], greater than the time (≈ 40 s) required to collect a complete set of EFM data. Because of the presence of a conductive substrate (here a silicon wafer with 10Ω cm resistivity), stored charges get screened by their substrate image, which forms a dipole located on the substrate surface. Its momentum is given at the lowest order by

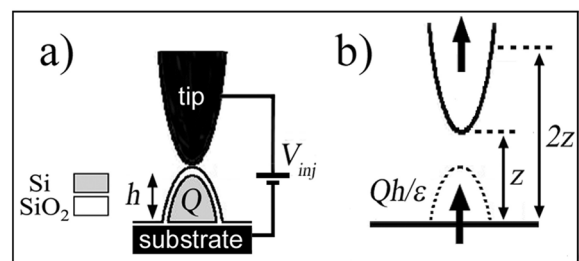


FIG. 1. (a) Injection of an amount Q of charges in a single silicon nanoparticle (gray) of height h by tunneling through the nanoparticle native oxide (white) from the EFM tip biased at V_{inj} . (b) Equivalent surface dipole $Q \times h/\epsilon$ (see text). When the tip is scanned at a distance z over the substrate plane, the dipole interacts with its tip image. In a plane geometry, this image dipole of momentum $Q \times h/\epsilon$ would be located at $2z$ over the substrate plane.

$Q \times h$, where h is the nanoparticle height, but this dipole is also screened by the nanoparticle dielectric medium (here with dielectric constant $\epsilon \approx 12$), leading to an effective surface dipole with equivalent momentum $Q \times h/\epsilon$. Dipole-dipole interactions then take place when scanning the nanoparticle in the EFM mode with the metallized cantilever tip apex located at a distance z over the substrate plane [see Fig. 1(b)]: the surface dipole interacts with its electrostatic image with respect to the metallized tip [see Fig. 1(b)], which would be located at a distance $2z$ over the substrate plane and of effective moment $Q \times h/\epsilon$ in a plane geometry approximation.

To detect this interaction, we perform EFM measurements which consist in recording the shift Δf of the cantilever resonance frequency with respect to its nominal frequency f_0 when the tip is oscillated in a linear pass at a fixed distance z over the substrate plane [Fig. 2(a)]. For $\Delta f \ll f_0$, the frequency shift Δf corresponds to a cantilever effective spring constant shift $\Delta k = 2k\Delta f/f_0$. Δk is the opposite of the gradient of electrostatic forces acting on the EFM cantilever tip. The distance z between the EFM tip apex and the substrate plane is set to $z \approx 100$ nm, thus discarding short-range surface forces in the EFM signals. Experiments were performed with a Nanoscope IIIA setup (Digital Instruments) working at atmospheric pressure, but in a dry nitrogen atmosphere to avoid anodic oxidation during the charge injection process and charge leakage through adsorbed water. We used a PtIr coated cantilever with nominal resonance frequency $f_0 = 53$ kHz, spring constant 2.2 N m^{-1} , and typical quality factor ≈ 200 .

The detection of dipole-dipole interactions is, in fact, not straightforward due to the weakness of the dipole-dipole force gradients compared to the usual capacitive or dipole-charge interactions [9] in EFM measurements. To distinguish between these features, EFM data are systematically studied as a function of the tip bias. We call V_{EFM} the voltage applied to the tip, and V_S the substrate potential. As the tip passes over the nanoparticle, one expects to measure three separate frequency shifts [10]. First, the increase of the tip-substrate capacitive force due to the presence of the nanoparticle of dielectric constant ϵ in the tip-substrate capacitor: this effect corresponds to an enhancement of the gradient of the attractive capacitive force, thus leading to a negative cantilever frequency shift Δf_ϵ proportional to $(V_{\text{EFM}} - V_S)^2$. Second, the interaction between stored charges and capacitive charges at the tip apex, of dipole-charge type, and giving rise to a shift proportional to $(V_{\text{EFM}} - V_S)$ and Q . This interaction has been used to map single charge fluctuations in CdSe nanocrystals at room temperature and in dry air [9]. Finally, the dipole-dipole interaction between the surface dipole associated with stored charges and its electrostatic tip image. It does not depend on V_S and can thus be observed when the tip is held at the substrate potential V_S . The generic property of dipole-dipole interactions is their scaling with the squared surface dipole $(Q \times h/\epsilon)^2$.

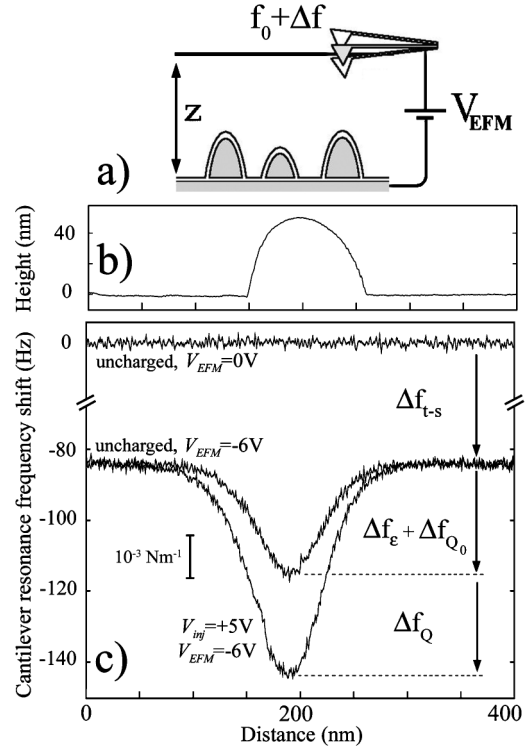


FIG. 2. (a) Schematics of EFM measurements: the cantilever is biased at V_{EFM} and oscillated at a constant distance z over the substrate plane. EFM data consist of the shift Δf of the cantilever resonance frequency f_0 . (b) Nanoparticle topography cross section. (c) EFM measurements at $V_{\text{EFM}} = 0$ and $V_{\text{EFM}} = -6$ V on the uncharged nanoparticle (with, however, an amount $Q_0 = -30e$ of native charges), showing the frequency shifts Δf_{t-s} and $\Delta f_\epsilon + \Delta f_{Q_0}$ with respect to the cantilever frequency $f_0 \approx 60$ kHz; and at $V_{\text{EFM}} = -6$ V after charge injection at $V_{\text{inj}} = +5$ V for 30 s, showing the additional charge shift Δf_Q (here $Q = +200e$). The distance between the tip apex and the substrate plane is $z = 96 \pm 2$ nm. The vertical scale bar indicates the correspondence between the frequency shifts and the cantilever effective spring constant shifts using $k = 2.2 \text{ N m}^{-1}$ and $f_0 = 53$ kHz. The gradient of forces acting on the EFM tip is the opposite of the cantilever spring constant shifts.

Experimental EFM signals are represented in Fig. 2(c). No frequency shift is detected for the 50 nm high nanoparticle imaged at $V_{\text{EFM}} = 0$ before charging. For $V_{\text{EFM}} \neq 0$, two signals take place. The first one is the frequency shift Δf_{t-s} associated with the tip-substrate capacitance. This negative frequency shift displays a parabolic behavior $(V_{\text{EFM}} - V_S)^2$, which enables one to measure the silicon substrate surface potential $V_S = +0.55$ V. The second shift $\Delta f_\epsilon + \Delta f_{Q_0}$ is associated with the nanoparticle. It essentially corresponds to the increase Δf_ϵ of the tip-substrate capacitance signal when the tip is scanned over the nanoparticle of dielectric constant $\epsilon \approx 12$, but also to a weak contribution Δf_{Q_0} of dipole-charge type [11], stemming from an amount $Q_0 = -30e$ of native charges in the nanoparticle. Finally, a shift Δf_Q is recorded after an injection of an amount Q of charges

inside the nanoparticle. Δf_Q reflects the dipole-charge interaction associated with the increase $Q \times h/\epsilon$ of the effective surface dipole moment after the charge injection, but also the dipole-dipole interactions associated with the total $(Q + Q_0) \times h/\epsilon$ effective surface dipole [12].

EFM signals are reported as a function of $V_{\text{EFM}} - V_S$ in Fig. 3(a). Before charging, only a weak amount $Q_0 = -30e$ of native charges are present in the nanoparticle, so that $\Delta f_\epsilon + \Delta f_{Q_0}$ values [solid line in Fig. 3(a)] stay negative within experimental accuracy (± 0.6 Hz), indicating that the tip-nanoparticle interaction mostly consists of capacitive force gradients. After charging $V_{\text{inj}} = +5$ V and $V_{\text{inj}} = -5$ V for 30 s [dashed and dotted lines in Fig. 3(a)], the $\Delta f_\epsilon + \Delta f_{Q_0} + \Delta f_Q$ curves become clearly asymmetric with respect to the surface potential V_S and reveal positive or negative frequency shifts (gradients of repulsive or attractive forces, respectively) for $|V_{\text{EFM}} - V_S| < 4$ V depending on the signs of V_{EFM} and V_{inj} . This regime corresponds to dipole-charge interactions greater than the nanoparticle capacitive interactions. It is used in practice to image surface dipoles with the EFM tip [8] at low $V_{\text{EFM}} - V_S$ values.

The charge signal Δf_Q is then obtained by subtracting $\Delta f_\epsilon + \Delta f_{Q_0}$ values from the EFM data of charged nanoparticles [see Fig. 3(b)]. Δf_Q values are found linear, with slopes $+3.7$ Hz/V (after charging at $V_{\text{inj}} = +5$ V) and -2.7 Hz/V (after charging at $V_{\text{inj}} = -5$ V). From the analysis of the ratio between charge to capacitive EFM signals [10], we deduce the corresponding $Q = +200e$ and $Q = -140e$ values for $V_{\text{inj}} = +5$ V and $V_{\text{inj}} = -5$ V, respectively [13]. Also, by monitoring the EFM signal at the surface potential ($V_{\text{EFM}} = 0.55$ V), we deduce the image force gradients associated with $Q_0 + Q$ [see the inset of Fig. 3(b)]: -1.5 Hz for $V_{\text{inj}} = -5$ V ($Q_0 + Q = -170e$) and -0.95 Hz for $V_{\text{inj}} = +5$ V ($Q_0 + Q = +170e$). Since these measurements average all Δf_Q data of Fig. 3(b), the experimental accuracy of the determination frequency shifts associated with dipole-dipole force gradients is ± 0.3 Hz.

We reported in Fig. 4 the frequency shifts associated with dipole-dipole interactions as a function of $Q + Q_0$. Measurements have been performed by successively injecting charges in the same nanoparticle as in Fig. 2 with injection biases in the range $-8 \leq V_{\text{inj}} \leq 8$ V and measuring dipole-dipole interactions with the procedure described in Fig. 3. These measurements demonstrate that our analysis properly separated dipole-charge and dipole-dipole interactions, since the dipole-dipole frequency shifts stay negative (gradient of an attractive force) within experimental accuracy (± 0.3 Hz) and irrespective of the sign of $Q + Q_0$. Also, the strength of dipole-dipole interactions is shown to quadratically depend on $(Q + Q_0) \times h/\epsilon$ as expected for this image force gradient.

Finally, we performed a numerical calculation of the dipole-dipole interactions associated with the nanopar-

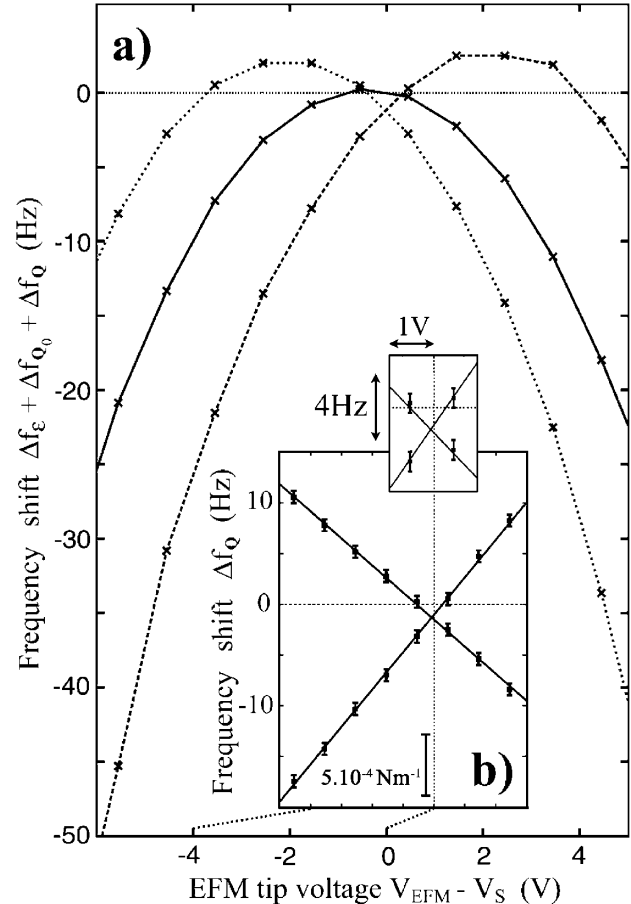


FIG. 3. (a) Cantilever frequency shift $\Delta f_\epsilon + \Delta f_{Q_0} + \Delta f_Q$ as a function of $V_{\text{EFM}} - V_S$ ($V_S = +0.55$ V) before (full line) and after charging at $V_{\text{inj}} = -5$ V and $+5$ V (dotted and dashed lines, respectively). Data were recorded within 40 s after charging. Lines are a guide to the eye. (b) Linear charge EFM signal Δf_Q , obtained by subtracting the EFM signals $\Delta f_\epsilon + \Delta f_{Q_0} + \Delta f_Q$ after and before the charging experiment. The solid line is a fit to the experimental data with slopes -2.7 Hz/V ($V_{\text{inj}} = -5$ V) and $+3.7$ Hz/V ($V_{\text{inj}} = +5$ V). This corresponds to $Q = -140e$ ($V_{\text{inj}} = -5$ V) and $Q = 200e$ ($V_{\text{inj}} = +5$ V), i.e., $Q_0 + Q = -170e$ and $+170e$, respectively, taking into account the $Q_0 = -30e$ native charge contribution [11]. Inset: zoom around the surface potential (vertical dotted line), evidencing the image force gradients: -1.5 ± 0.3 Hz for $Q_0 + Q = -170e$ and -0.95 ± 0.3 Hz for $Q_0 + Q = +170e$.

ticle. To do so, we solved in a cylindrical geometry the Poisson equation using finite elements and calculated the force and force gradients between an EFM tip and the nanoparticle [10]. The tip is here modeled as a conical tip with half-angle 25° and hemispherical apex with radius 15 nm. From the topography data of Fig. 2(a), the nanoparticle is described as hemiellipsoidal with base radius 40 nm and height 50 nm. Calculations enable one to calculate Δf_{t-s} , Δf_ϵ , and Δf_Q EFM data as a function of $V_{\text{EFM}} - V_S$. These frequency shifts are deduced from force gradients using the EFM cantilever spring constant k as the single adjustable parameter. In practice, we used

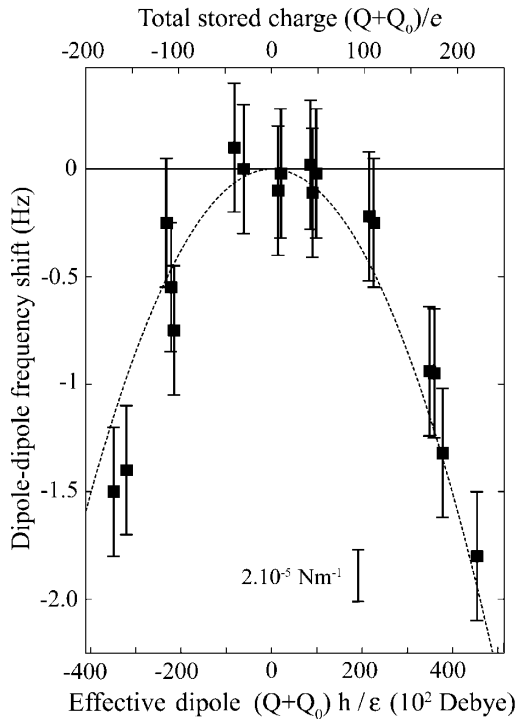


FIG. 4. Points: frequency shift associated with dipole-dipole interactions, plotted as a function of the effective surface dipole momentum $(Q + Q_0)/\epsilon$ associated with the total stored charge $Q + Q_0$. Dashed line: numerical calculation of the dipole-dipole interaction frequency shift as a function of $Q + Q_0$ (see the text).

$k = 2.2 \text{ N m}^{-1}$. This value is fixed by comparing experimental and calculated Δf_{i-s} values. It is then checked that the calculation of Δf_ϵ and of the slope of Δf_Q data as a function of $V_{\text{EFM}} - V_S$ fall in quantitative agreement with experimental EFM measurements. We finally calculate dipole-dipole interactions by calculating Δf_Q for $V_{\text{EFM}} = V_S$, and predict a -1.15 Hz frequency shift for $|Q_0 + Q| = 170e$, in agreement with the measured values from Fig. 3 within experimental uncertainty. In Fig. 4, we show the full comparison between numerically calculated (dotted line) and experimental (points) dipole-dipole interactions as a function of the dipole moments generated by the charge injection in the nanoparticle. This clearly demonstrates the quadratic behavior of the dipole-dipole interaction with respect to the momentum of the surface dipole.

These results bring clear evidence for dipole-dipole interactions associated with nanostructures. This has been achieved at room temperature in dry nitrogen atmosphere experiments using artificial dipoles with tunable effective moments in the 10^3 – 10^4 D range created by injection of out-of-equilibrium carriers in single silicon nanoparticles. Such an “open loop” spectroscopic analysis of electrical forces can apply to noncontact atomic force microscopy in an ultrahigh vacuum environment. Taking advantage of the much closer tip-substrate distances, it could enable one to identify and measure the

strength of short-range electrostatic interactions associated, e.g., with molecular dipoles or atomic-scale charge displacements [5] on surfaces. This makes electric force microscopy very promising to probe dipolar interactions at the nanoscale.

We are indebted to J. P. Nys, Y. M. Niquet, G. Allan, and C. Delerue for technical help and fruitful discussions. This work is supported by a “Nanostructures” ACI grant and in part by the European Community’s Human Potential Programme under Contract No. HPRN-CT-2002-00320, NANOSPECTRA.

*Electronic address: thierry.melin@isen.fr

- [1] M. Böhringer, K. Morgenstern, W. D. Schneider, R. Berndt, F. Mauri, A. De Vita, and R. Car, *Phys. Rev. Lett.* **83**, 324 (1999).
- [2] T. Yokoyama, S. Yokoyama, T. Kamikado, Y. Okuno and S. Mashiko, *Nature (London)* **413**, 619 (2001).
- [3] L. S. Li and A. P. Alivisatos, *Phys. Rev. Lett.* **90**, 097402 (2003).
- [4] A. L. Shluger, A. I. Livshits, A. S. Foster and C. R. A. Catlow, *J. Phys. Condens. Matter* **11**, R295 (1999).
- [5] M. A. Lantz, H. J. Hug, R. Hoffmann, S. Martin, A. Baratoff, and H. J. Güntherodt, *Phys. Rev. B* **68**, 035324 (2003).
- [6] Y. Martin, C. C. Williams, and H. K. Wickramasinghe, *J. Appl. Phys.* **61**, 4723 (1987).
- [7] E. A. Boer, L. D. Bell, M. L. Brongersma, H. A. Atwater, M. L. Ostraat, and R. C. Flagan, *Appl. Phys. Lett.* **78**, 3133 (2001).
- [8] T. Mélin, D. Deresmes, and D. Stiévenard, *Appl. Phys. Lett.* **81**, 5054 (2002).
- [9] Todd D. Krauss and Louis E. Brus, *Phys. Rev. Lett.* **83**, 4840 (1999).
- [10] T. Mélin, H. Diesinger, D. Deresmes, and D. Stiévenard, *Phys. Rev. B* **69**, 035321 (2004).
- [11] The dipole-charge and dipole-dipole interactions associated with Q_0 are obtained by removing from $\Delta f_\epsilon + \Delta f_Q$ values measured as a function of $V_{\text{EFM}} - V_S$ the capacitive part Δf_ϵ proportional to $(V_{\text{EFM}} - V_S)^2$. This leads to a signal linear with $V_{\text{EFM}} - V_S$ with a -0.6 Hz/V slope corresponding to the $Q_0 = -30e$ value, with no measurable dipole-dipole interactions.
- [12] Experimentally, dipole-dipole interactions associated with Q_0 are negligible [11].
- [13] The formula for $\mathcal{R} = \Delta f_\epsilon / \Delta f_Q$ in Ref. [10] is given neglecting image force gradients. To apply this model here, one needs (i) to subtract dipole-dipole interactions from experimental Δf_Q data and (ii) to correct the uncharged particle EFM signals from the effect of the amount Q_0 of native charges, which can be simply done by averaging $\Delta f_\epsilon + \Delta f_{Q_0}$ values measured for $V_{\text{EFM}} - V_S$ and $-V_{\text{EFM}} - V_S$, because image force gradients associated with Q_0 are negligible. Experimentally, we hence determine $\mathcal{R} = -1.05$ ($V_{\text{inj}} = +5 \text{ V}$) and $\mathcal{R} = 0.73$ ($V_{\text{inj}} = -5 \text{ V}$) for a detection bias $V_{\text{EFM}} = +4 \text{ V}$. Applying the model from Ref. [10], we deduce $Q = +200e$ and $Q = -140e$ for $V_{\text{inj}} = +5 \text{ V}$ and $V_{\text{inj}} = -5 \text{ V}$, respectively.